Journal of Ceramic Processing Research. Vol. 18, No. 2, pp. 141~145 (2017)

J O U R N A L O F
Ceramic Processing Research

Effect of the silica particle diameter on the morphology of catalyst layer in proton exchange membrane fuel cells

Eun Kwang Jang[a], Sang Bin Lee[a], Tae-Hyun Kim[a] and Sung-Chul Yi[a,b,*]

[a]*Department of Chemical Engineering, Hanyang University, Haengdang-dong, Seongdong-gu, Seoul 133-791, Korea*
[b]*Department of Hydrogen and Fuel Cell Technology, Hanyang University, Haengdang-dong, Seongdong-gu, Seoul 133-791, Korea*

Providing sufficient hydration in a proton exchange membrane fuel cell is important to obtain high fuel-cell performance under a low relative humidity (RH) condition. Herein, we investigated the influence of the silica (SiO_2) particles on the agglomerated structure in the catalyst layer (CL). The CLs were prepared with three different particle diameters namely 8, 30 and 100 nm and their water uptake (WU) behavior and the electrochemical properties were subsequently characterized. As a result, the CL containing 8 nm SiO_2 particles showed intimate contact between the SiO_2 particles and Nafion ionomer, thereby improving the electrochemical surface area and WU behavior. Consequently, it is clearly demonstrated that the cell polarization of the 8 nm SiO_2-containing CL presented 1.042 A cm^{-2} at 0.5 V under 20% RH condition, which exhibited 2.94 times higher than that of the CL without the addition of SiO_2.

Key words: Proton exchange membrane fuel cell, Relative humidity, Catalyst layer, Silica, Water uptake.

Introduction

A proton exchange membrane fuel cell (PEMFC) is a highly efficient and eco-friendly energy-conversion device to minimize contamination which is expected as one of the most promising alternatives to conventional fossil fuel. For the purpose of utilizing atmospheric air as an oxidizing agent in the PEMFC, a stable and improved performance has to be considered and carried out in a wide range of relative humidity (RH) [1]. However, the PEMFC requires an external humidification for sufficient hydration in typical perfluorosulfonic acid membranes due to the dependence of proton transport mechanism on the water uptake (WU) [2]. To commercialize the PEMFCs, the system integrators focused on producing a membrane electrode assembly (MEA) which can produce at least 1.5-2.0 A cm^{-2} at 0.6 V with a platinum (Pt) loading of 0.125 mg cm^{-2} under 0-100% RH conditions [3]. Therefore, the WU in the MEA is the critical issue for successful commercialization and increase cell performance under low RH conditions.

For several decades, numerous researchers [4-24] have investigated on improving the WU to achieve high fuel-cell performance under low RH conditions. Watanabe et al. [4,5] firstly reported an improved concept of the self-humidifying proton exchange membrane containing metal-oxide particles and Pt catalyst, which retained the WU and initiated the chemical oxidation of H_2 and O_2, respectively. Since then, the self-humidifying membranes have been extensively explored to improve the WU of the membrane [6-13]. On the other hand, a number of models of the self-humidifying catalyst layers (CLs) [14-24], generally including the hygroscopic additives, have been recently manufactured owing to dehydration of the anode CL by the electro-osmotic drag. Han et al. [14] reported improved cell polarization under low RH by fabricating thin silica (SiO_2)-Nafion functional layer between the Nafion membrane and the CL. However, the MEA deteriorated the cell polarization under sufficient humidification compared to that of the conventional one due to the increased ohmic resistance. Hence, Inoue et al. [15, 16] have studied a simple fabrication method of the SiO_2-containing CL, which controls both hydrolysis/condensation of SiO_2 suspension and the catalyst ink in a single vial. These authors suggested that the electrochemical surface area (ECSA) was improved as increasing the SiO_2 content. However, others [17, 18] reported the decreased ECSA because the SiO_2 insulates the electrocatalytic sites of the Pt. On the other hand, Han et al. [14] and Inoue et al. [16] have asserted that SiO_2-containing CL has reduced the performance fluctuation under not only low RH but also high RH condition. Although the CLs with the addition of hygroscopic additives have been extensively studied, the effects of the hygroscopic additives on the CL morphology and thereby the cell polarization are ambiguous so far.

The interface between the SiO_2 particle and the Nafion ionomer is important to the WU behavior of CL. Hence, the dynamic vapor sorption (DVS) experiment

*Corresponding author:
Tel : +82-2-2220-0481
Fax: +82-2-2298-5147
E-mail: scyi@hanyang.ac.kr

was implemented to precisely understand the relation between the morphology and the WU of the CL. Subsequently, the impacts of the different SiO_2 particle sizes on the cell polarizations under low RH condition were examined. The cyclic voltammetry (CV) was further employed to correlate the agglomerate structure and the electrochemically available surface area. Hence, an attempt was made in this paper to study the effect of hygroscopic additives namely SiO_2-containing CL by varying the particle diameter as a function.

Experimental

Materials

20 wt% carbon-supported platinum (Pt/C) catalyst and 40 wt% tetrabutylammonium hydroxide (TBAOH) were purchased from Alfa Aesar. The ammonia, 1-propanol, methanol, tetraethyl orthosilicate (TEOS), glycerol and 1,5-pentanediol were purchased from Sigma Aldrich. The Nafion membrane and 5 wt% Nafion dispersion were purchased from Ion Power. For the electrochemical characterizations, the three-serpentine cell fixture with an area of 9 cm^2 was purchased from CNL Corp. and the gas diffusion layer with the microporous layer (GDL 10BC) was prepared from Sigracet.

Preparation of the membrane electrode assemblies

The catalyst inks used in this study were prepared as following manner. In a vial equipped with a magnetic stirrer (50 mL), 2.24 g of the 5 wt% Nafion dispersion was added into 3.1 g of glycerol followed by homogenization. After then, the TBAOH was added followed by 30 h stirring. For the SiO_2-containing CL, the prepared 10 wt% colloidal SiO_2 solution was applied into the catalyst ink with the SiO_2-to-carbon ratio 0.04. The SiO_2 particles with different sizes (8 nm, 30 nm and 100 nm particles) were synthesized by Stöber method [25, 26]. Briefly, 1.2 g of TEOS was added into a 3.0 M ammonia solution in a mixture of 1-propanol and methanol. The solution was stirred in room temperature to form spherical colloidal SiO_2 through the sol-gel reaction. After the reaction, the solution was centrifuged and washed and dried in a vacuum oven at 50 °C for 24 hrs. Then, 10 wt% aqueous solutions of SiO_2 with different sizes namely 8, 30 and 100 nm were prepared before use.

The 0.3 T polytetrafluoroethylene (PTFE) film was cleansed and repeatedly painted with the catalyst ink and annealed in a convection oven at 130 °C until the Pt loading reached 0.2 mg cm^{-2}. Subsequently, a sufficient amount of 1,5-pentanediol was applied onto the CL surface to increase decal transfer rate. Before the decal transfer, the Nafion membrane was transformed into sodium-form by boiling the membrane in an aqueous sodium hydroxide (1 wt%). After that, the decal was assembled by sandwiching the sodium-form Nafion membrane and hot-pressing at 140 °C for 5 min [26]. To prevent severe delamination, the PTFE cover surrounding the decal was removed after successful transfer of CL. After peeling off the PTFE films, the MEA was boiled in deionized water at 100 °C to remove the residual solvents and 0.5 M sulfuric acid solution at 80 °C and finally cleansing in boiling water for 1 h before use.

Characterizations

The scanning electron microscopy (SEM, Hitachi S-4800) was conducted to examine the microstructure of CL. The WU behavior as a function of RH was identified by conducting the DVS experiment (Advantage Surface Measurement Systems). The MEA was cut into a size of 50 mm^2. All the MEA samples were equilibrated under 0% RH of N_2 feed at 25 °C for 2 hrs or more until the mass variation rate reached 0.002 wt% min^{-1} to determine the initial weight. After the equilibrium, the MEA was hydrated up to 90% RH by stepwise increasing the RH of N_2 feed by 15% RH, followed by dehydrating down to 0% RH as same manner [27]. All the MEA samples were stabilized at each RH step for at least 30 min to ensure steady-state results. The WU of Nafion membrane was obtained to subtract the water content of membrane from the total amount of water absorbed by the MEA samples. The water content was calculated based on the mass change of sample.

The cell polarization was evaluated with a 9 cm^2 single-serpentine cell fixture. The 99.999% of H_2 and O_2 gas feed were provided into the cell at 70 °C and ambient pressure, while the humidifying temperature was fixed to reach the target RH. To obtain the CV profiles, the H_2 and N_2 gas feed were added to the cell with a fixed flow rate of 20 sccm, while the cell and humidification temperature was maintained at 30 °C [28]. The potential was cycled from 0.05 V to 1.20 V with a scan rate of 50 mV s^{-1}. The amount of charge involved in atomic hydrogen adsorption was used to calculate the ECSA.

Results and Discussion

Morphology of the SiO_2-containing CLs

Fig. 1 shows the SEM images of CL surfaces prepared from different particle sizes of SiO_2. As seen in Fig. 1(a), the 8 nm SiO_2-containing CL presented the well-dispersed and well-contacted Pt/C-SiO_2-Nafion agglomerate structure compared to that of the CLs with larger diameters of the SiO_2 particles. For the CLs containing larger sizes of SiO_2, the SiO_2 particles were often observed as unconnected and dis-continuous particles from the Pt/C-Nafion agglomerates. In addition, the Pt/C-Nafion agglomerates showed severely aggregated morphology as increasing the SiO_2 particle diameter. Recently, for larger SiO_2-containing CLs, the poorly contacted Pt/C-Nafion agglomerate structures were also identified by Lee et al. [29]. From the SEM images, the

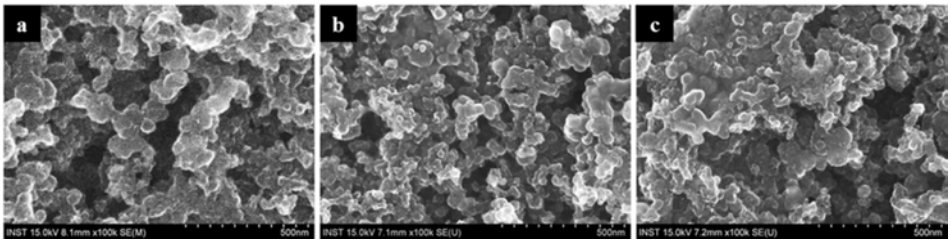

Fig. 1. SEM images of the SiO_2-containing CLs with different SiO_2 particle diameters. (a) 8 nm SiO_2, (b) 30 nm SiO_2 and (c) 100 nm SiO_2.

CL prepared with the small size of SiO_2 particles may enhance the WU and ECSA due to intimate contact between the SiO_2 particles and Nafion ionomer. For the CLs with larger SiO_2 particle size, the ohmic resistance may be increased invariantly by the decrease of charge-transfer pathways because of the weak contact among the agglomerates.

Water uptake of the SiO_2-containing CL

The WU behavior of SiO_2-containing CL can be varied due to difference in the interfaces between the SiO_2 particles and Nafion ionomer. Fig. 2 presents the water sorption isotherms of the CLs prepared with different SiO_2 particle diameters. As observed in Fig. 2, the SiO_2-containing CLs showed higher WU than the CL without the addition of SiO_2 particles because of the hygroscopic characteristic of SiO_2. Especially, the 8 nm SiO_2-containing CL showed highest WU compared to that of the other CLs, indicating that both the hygroscopic characteristic of SiO_2 and the morphology of Pt/C-SiO_2-Nafion agglomerate affect the WU behavior. For the small-sized SiO_2 particles relative to the Nafion covering layer, the close contact between the SiO_2 particles and Nafion ionomer can be obtained due to the penetration of SiO_2 particles into the Pt/C-Nafion agglomerate. In addition, the intimate interface between the SiO_2 particle and Nafion ionomer showed the less-clustered agglomerate structure, indicating severely segregated Nafion agglomerates. Hence, weakly clustering of Nafion agglomerate can be enhanced the WU of CL owing to high degree of phase separation. It can be deduced that the morphology of the Pt/C-SiO_2-Nafion agglomerate significantly affects the water sorption behavior.

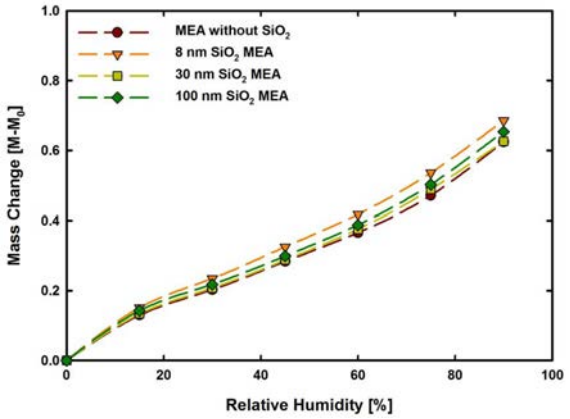

Fig. 2 Water-uptake behaviors of the MEA without SiO_2 and SiO_2-containing MEAs with different SiO_2 particle diameters.

Electrochemical performances of the SiO_2-containing MEA

Fig. 3 presents the cell polarizations of the MEAs at different RH conditions. All the MEAs were characterized with H_2/O_2 feed gas at the anode/cathode flow channel under 100% RH and 20% RH conditions. For 100% RH operation, the cell polarization was slightly decreased as increasing the SiO_2 particle size, indicating the increase of ohmic resistance due to the non-conductive SiO_2 particles separated from the agglomerates. Specifically, the cell performance of the 8 nm SiO_2-containing MEA was improved compared to that of the 100 nm SiO_2-containing MEA owing to the well-contacted Pt/C-

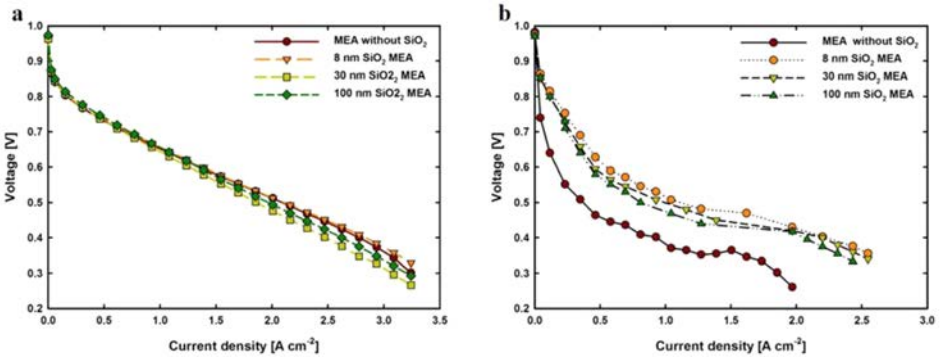

Fig. 3 Cell polarizations of the MEA without SiO_2 and SiO_2-containing MEAs with different SiO_2 particle diameters. (a) 100% RH operation and (b) 20% RH operation.

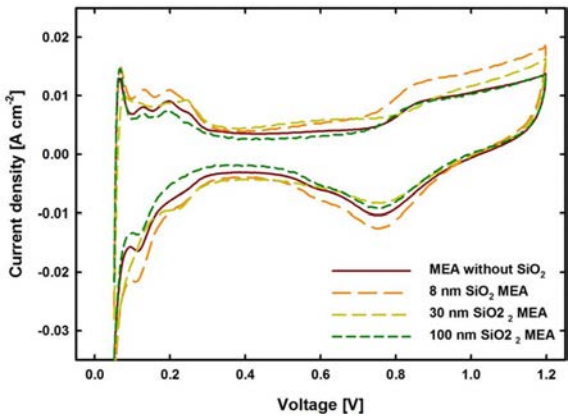

Fig. 4 Cyclic voltammetry of the MEA without SiO_2 and SiO_2-containing MEAs with different SiO_2 particle sizes.

SiO_2-Nafion agglomerate structure. Under 20% RH condition, a typical type of cell voltage decrease in the low-current region [30] was obtained for all MEAs. Overall, the MEAs with SiO_2 particles improved the cell polarization due to hygroscopic characteristic of SiO_2. Specifically, the cell performance of the 8 nm SiO_2-containing MEA has significantly improved by exhibiting 1.042 A cm^{-2} at 0.5 V which presented 2.94 and 1.51 times higher than the MEA without SiO_2 and 100 nm SiO_2-containing MEA, respectively. As observed in the SEM image (Fig. 1), the sufficiently small-sized SiO_2 particles in the agglomerate have a great contact with Nafion electrolyte, hence providing low ohmic resistance under low RH condition. Consequently, the Pt/C-Nafion agglomerate structure with break-in SiO_2 particles improves the cell polarizations under both high and low RH conditions.

Fig. 4 presents the CV plots of the MEAs to examine the influence of the SiO_2 particle size on the ECSA. As observed in Fig. 4, the 8 nm SiO_2-containing MEA presented the highest ECSA of 68.5 m^2 g^{-1}, which showed higher than that of the MEA without SiO_2 (50.7 m^2 g^{-1}). On the other hand, the MEAs containing the 30 nm and 100 nm SiO_2 particle diameters exhibited the decrease in the ECSA of 49.3 and 46.2 m^2 g^{-1}, respectively. As observed from SEM images (Fig. 1), the size and morphology of the agglomerates were significantly affected as the SiO_2 particles approach among the agglomerates. In addition, the intimate contact between the SiO_2 particles and Nafion ionomer in the 8 nm SiO_2-containing CL contributed to increased WU and electrochemical performances. Therefore, it is important to enhance the CL structure by efficiently penetrate the SiO_2 particles inside the agglomerates.

Conclusions

This paper reports the improvement of the PEMFC performance under 20% RH condition by tailoring the morphology of Pt/C-SiO_2-Nafion agglomerate. The CLs with different particle sized SiO_2 viz., 8, 30 and 100 nm were prepared and examined for their interface between the SiO_2 particle and Nafion ionomer. Among the synthesized SiO_2 particle diameters, the 8nm SiO_2-containing CL showed the well-dispersed and well-contacted morphology due to penetration of the SiO_2 particles into the Pt/C-Nafion agglomerate. The water sorption experiment revealed that the 8 nm SiO_2-containing CL improved the WU behavior compared to that of the CLs containing larger sizes of SiO_2 owing to intimate contact between SiO_2 particles and Nafion ionomer. As a result, the 8 nm SiO_2-containing MEA presented the improved cell polarization under low RH condition with 2.94-fold current density at 0.5 V compared to that of the MEA without SiO_2 particles. Therefore, fabrication of the improved agglomerate structure is mandatory to enhance the cell polarization at low RH operation.

Acknowledgments

This research was supported by the Ministry of Trade, Industry & Energy (MOTIE), Korea Institute for Advancement of Technology (KIAT) through the Encouragement Program for the Industries of Economic Cooperation Region.

References

1. R. Devanathan, Energy Environ. Sci. 1 (2008) 101-119.
2. C. Siegel, Energy 33 (2008) 1331-1352.
3. MK. Debe, Nature 486 (2012) 43-51.
4. M. Watanabe, H. Uchida, Y. Seki, M. Emori and P. Stonehart, J. Electrochem. Soc. 143 (1996) 3847-3852.
5. M. Watanabe, H. Uchida and M. Emori, J. Electrochem. Soc. 145 (1998) 1137-1141.
6. B. Yameen, A. Kaltbeitzel, A. Langer, F. Muller, U. Gosele, W. Knoll and O. Azzaroni, Angew Chem. Int. Ed. 48 (2009) 3124-3128.
7. W. Han and KL. Yeung, Chem. Commun. 47 (2011) 8085-8087.
8. J. Wang, Z. Zhang, X. Yue, L. Nie, G. He, H. Wu and Z. Jiang, J. Master. Chem. A1 (2013) 2267-2277.
9. Y. Zhang, H. Zhang, X. Zhu and C. Bi, J. Phys. Chem. B 111 (2007) 6391-6399.
10. E.D. Wang, P.F. Shi and C.Y. Du, J. Power Sources 175 (2008) 183-188.
11. R. Eckl, W. Zehtner, C. Leu and U. Wagner, J. Power Sources 138 (2004) 137-144.
12. W. Zhang, MKS. Li, PL. Yue and P. Gao, Langmuir 24 (2008) 2663-2670.
13. H. Zarrin, D. Higgins, Y. Jun, Z. Chen and M. Fowler, J. Phys. Chem. C 115 (2011) 20774-20781.
14. M. Han, S.H. Chan and S.P. Jiang, Int. J. Hydrogen Energy 32 (2007) 385-391.
15. N. Inoue, M. Uchida, M. Watanabe and H. Uchida, Electrochem. Commun. 16 (2012) 100-102.
16. N. Inoue, M. Uchida, M. Watanabe and H. Uchida, Electrichim. Acta 88 (2013) 807-813.
17. H.N. Su, L.J. Yang, S.J. Liao and Q. Zeng, Electrochi. Acta 55 (2010) 8894-8900.

18. H. Matsumori, S. Takenaka, H. Matsune and M. Kishida, Appl. Catal. A Gener 373 (2010) 176-185.
19. U.H. Jung, K.T. Park, E.H. Park and S.H. Kim, J. Power Sources 159 (2006) 529-532.
20. H. Su, L. Xu, H. Zhu, Y. Wu, L. Yang, S. Liao, H. Song, Z. Liang, and V. Birss, Int. J. Hydrog Energy 35 (2010) 7874-7880.
21. H. Liang, L. Zheng and S. Liao, Int. J. Hydrogen Energy 37 (2012) 12860-12867.
22. I.S. Choi, K.G. Lee, S.G. Ahn, D.H. Kim, O.J. Kwon and J.J. Kim, Catal. Commun. 21 (2012) 86-90.
23. H. Liang, D. Dang, W. Xiong, H. Song and S. Liao, J. Power Sources 241 (2013) 367-372.
24. Z. Miao, H. Yu, W. Song, D. Zhao, L. Hao, B. Yi and Z. Shao, Electrochem. Commun. 11 (2009) 787-790.
25. W. Stober, A. Fink and E. Bohn, J. Colloid Interface Sci. 26 (1968) 62-69.
26. C.Y. Jung, J.Y. Yi and S.C. Yi, Energy 68 (2014) 794-800.
27. C.Y. Jung and S.C. Yi, Electrochem. Commun. 35 (2013) 34-37.
28. R.N. Carter, S.S. Kocha, F.T. Wagner, M. Fay, H.A. Gasteiger, ECS Trans. 11 (2007) 403-410.
29. Y. Lee, T.K. Kim and Y.S. Choi, Fuel Cells 13 (2013) 173-180.
30. C.Y. Jung, T.H. Kim and S.C. Yi, Chem. Sus. Chem. 7 (2014) 466-473.